HHS Public Access

Author manuscript

*Nat Struct Mol Biol*. Author manuscript; available in PMC 2012 July 01.

Published in final edited form as:

*Nat Struct Mol Biol*. ; 19(1): 122–127. doi:10.1038/nsmb.2190.

# A METAL SWITCH FOR CONTROLLING THE ACTIVITY OF MOLECULAR MOTOR PROTEINS

**Jared C. Cochran**[1,2], **Yu Cheng Zhao**[1], **Dean E. Wilcox**[1], and **F. Jon Kull**[1]

[1]Dartmouth College, Department of Chemistry, Hanover, New Hampshire 03755, USA

## Abstract

Kinesins are molecular motors that require a divalent metal ion (e.g., $Mg^{2+}$) to convert the energy of ATP hydrolysis into directed force production along microtubules. Here we present the crystal structure of a recombinant kinesin motor domain bound to $Mn^{2+}$ and ADP, and report on a serine to cysteine substitution in the switch 1 motif of kinesin that allows its ATP hydrolysis activity to be controlled by adjusting the ratio of $Mn^{2+}$ to $Mg^{2+}$. This mutant kinesin binds ATP similarly in the presence of either metal ion, but its ATP hydrolysis activity is greatly diminished in the presence of $Mg^{2+}$. In several different members of the kinesin superfamily, this defect is rescued by $Mn^{2+}$, providing a way to control both the enzymatic activity and force generating ability of these nanomachines.

## INTRODUCTION

Purine nucleotide-binding proteins, including small monomeric G-proteins, protein-synthesizing GTPases (elongation factor), heterotrimeric G-proteins, thymidine kinases, RNA helicases (CSFV NS3 helicase), rad50, RecA, myosin, dynein, and kinesin superfamilies, constitute a large portion of the hydrolases (EC 3.6) found in biological systems. These enzymes are crucial for a diverse range of cellular processes, but all use a phosphate-binding loop (P-loop or Walker A motif; consensus sequence GxxxxGKS/T) to bind the nucleotide phosphates and all require a metal ion (typically magnesium, $Mg^{2+}$) in the active site [reviewed in [1]]. The metal ion coordination usually includes a conserved serine or threonine in the P-loop, an oxygen of the β-phosphate, and two water ligands. The



Correspondence to: F. Jon Kull, PhD, 6128 Burke Laboratory, Hanover, NH 03755, USA, Tel.: 603-646-1552, Fax: 603-646-3946, F.Jon.Kull@Dartmouth.edu.

[2]Current address is Indiana University, Department of Molecular and Cellular Biochemistry, Simon Hall 400B, 212 S. Hawthorne Dr., Bloomington, IN 47405, USA.

**ACCESSION CODES**

Atomic coordinates and structure factors for the reported crystal structure have been deposited with the Protein Data Bank under the accession code 3PXN.

**AUTHOR CONTRIBUTIONS**

J.C.C. cloned constructs, purified protein, crystallized, collected, processed and refined X-ray data with help from Y.C.Z.. J.C.C. performed kinetic assays, analyzed kinetic data, performed EPR experiments, conducted MT gliding assays, and wrote the paper. D.E.W. and F.J.K were involved in study conception, study design, and editing final manuscript. All authors discussed the results and commented on the manuscript. The authors declare that they have no competing interests as defined by Nature Publishing Group, or other interests that might be perceived to influence the results and/or discussion reported in this article.

remaining two ligands required to satisfy the octahedral coordination geometry vary depending on whether nucleotide diphosphate or triphosphate occupies the site. Therefore, the metal ion anchors an intricate network of interactions in the enzyme that are believed to be necessary to lower the free energy of the transition state and achieve an enhanced rate of hydrolysis.

Molecular motors, such as kinesins and myosins, as well as molecular switches, such as G-proteins, utilize the energy from nucleotide hydrolysis to perform various cellular tasks. In addition to the P-loop, these proteins use similar structural motifs to sense and respond to the presence or absence of the γ-phosphate of the nucleotide called switch 1 and switch 2 (NxxSSR and DxxGxE are consensus sequences in kinesins and myosins, respectively) and coordinate nucleotide hydrolysis[2]. In contrast to these structural similarities, there are major differences in the mechanistic timing for the “closing” and “opening” of these switches around the nucleotide during the NTPase cycle. The conformational changes of the switches are propagated beyond the active site to relay a structural signal that conveys the state of the nucleotide bound to the enzyme[3]. A complete understanding of the mechanisms of nucleotide binding and hydrolysis requires a detailed description of these conformational changes and other molecular interactions within the active site that initiate force production in molecular motors or turn a molecular switch “on” and “off”.

Thio-substitution and metal ion rescue experiments were developed to characterize the metal catalyzed reactions of different classes of ribozymes [reviewed in [4]]. This provided a powerful and direct probe of catalytically important metal-nucleotide interactions within RNA macromolecules[5–8], as well as protein-based enzymes such as DNA transposases[9–11]. $Mg^{2+}$ is a relatively hard metal ion (high charge density, low polarizability) that participates in catalysis through coordination of oxygens from hydroxyls and/or phosphates. In previous metal rescue experiments, oxygen was substituted with sulfur, which does not bind as tightly to $Mg^{2+}$ but has a higher affinity for softer transition metal ions with lower charge density and somewhat greater polarizability, such as $Mn^{2+}$ or $Zn^{2+}$[(ref. 12)]. Therefore, in previous studies, the addition of $Mn^{2+}$ resulted in the catalytic “rescue” of the sulfur-substituted macromolecule, which provided evidence for metal binding sites that are required for the catalytic activity of many different ribozymes[4].

In this study, we set out to develop a similar strategy to probe metal interactions within kinesin molecular motors by taking advantage of the differential affinities of $Mg^{2+}$ and $Mn^{2+}$ for serine (−OH) and cysteine (−SH) amino acids. Substitution of an active site serine with cysteine is expected to diminish catalytic activity if the serine interaction with $Mg^{2+}$ is critical for catalysis. Substituting $Mg^{2+}$ with $Mn^{2+}$, which interacts more strongly with cysteine, should therefore restore the metal interaction with this residue, thus rescuing catalysis.

## RESULTS

### Kinesin•MnADP structure shows that $Mn^{2+}$ replaces $Mg^{2+}$

In the present study, we have investigated monomeric and dimeric proteins of different kinesin families (Kin1, Kin5, Kin10, and Kin14) to characterize our metal switch technology

across the superfamily. As with other protein-based systems, certain kinesin proteins afford the ability to answer different structural, biochemical, and mechanistic questions related to the ATPase cycle given their unique biophysical properties. In this manuscript, monomeric Kin5 (Eg5) was predominantly used for biochemical assays since this motor can be purified nucleotide-free without loss of stability or activity[13]. This kinesin provides the ideal model system for designing specific experiments to assess the complex ATPase mechanism of kinesin motors in the presence of different metals such as $Mg^{2+}$ or $Mn^{2+}$. However X-ray crystallographic studies and *in vitro* MT motility assays were conducted using Kin10 (Nod) and Kin1 (conventional kinesin), respectively.

We began by purifying and crystallizing the motor domain of a *Drosophila melanogaster* kinesin (Nod) with $Mn^{2+}$ and ADP in order to solve its high resolution structure using X-ray crystallography. The identity of the bound metal in our kinesin crystals was determined by electron paramagnetic resonance (EPR) spectroscopy (Fig. 1a) and $F_oF_c$ difference mapping using the Kin10•MgADP model for initial refinement (Fig. 1b)[14]. EPR data for the washed and denatured crystalline sample had the distinctive six-peak spectrum typical of $Mn^{2+}$ and a positive density peak in the $F_oF_c$ map was observed at the metal binding site. The Kin10•MnADP structure was refined to 2.6 Å (Table 1; Supplementary Figure 1) and aligned with Kin10•MgADP with a root mean square deviation (RMSD) at 0.32 $Å^2$ (Fig. 1c), suggesting that the overall structure was very similar, despite $Mn^{2+}$ being bound at the active site. The $Mn^{2+}$ ion showed octahedral oxygen coordination consisting of the nucleotide β-phosphate, the P-loop serine and four waters (Fig. 1d,e).

## Switch 1 substitution shows similar metal and ATP binding

Wild-type kinesins have a conserved serine in switch 1 (NxxS**S**R) that is thought to coordinate the metal during ATP hydrolysis (Fig. 1f)[15]. Site-directed mutagenesis was used to replace this metal-interacting serine residue in human Kin5(WT) with cysteine [Kin5(SC)]. Since EPR signals from $Mn^{2+}$ bound to proteins are often not observed at common X-band frequencies[16], EPR detection of free $Mn^{2+}$ was used to monitor $Mn^{2+}$ binding to Kin5(WT) and Kin5(SC) (Fig. 2a; Supplementary Fig. 2). Similar weak binding of MnADP (reduced free $Mn^{2+}$ signal), which was displaced by excess $Mg^{2+}$, was found with both enzymes. These results indicate that the switch 1 serine-to-cysteine substitution does not alter metal binding in the presence of ADP.

Similar rates of MgATP or MnATP binding to Kin5(WT) and Kin5(SC) were observed by monitoring changes in intrinsic tryptophan fluorescence, which changes upon ATP binding (Fig. 2b)[13]. When these experiments were performed as a function of ATP concentration, the overall ATP affinity was comparable for Kin5(WT) with $Mg^{2+}$ or $Mn^{2+}$ ($K_{d,ATP}$ = 6.2 μM and 2.5 μM, respectively; Fig. 2c). However, for Kin5(SC) the binding affinity was slightly weakened with $Mg^{2+}$ or $Mn^{2+}$ (10.4 μM and 21.7 μM, respectively). When comparing the amplitudes of each transient as a function of ATP concentration, differences in the overall thermodynamics for substrate binding were observed (Fig. 2d), indicating a substantial change in the SC kinesin ATPase cycle downstream from the MgATP-dependent isomerization of the enzyme.

### Kinesin activity controlled using $[Mn^{2+}]/[Mg^{2+}]$ ratio

The steady-state ATPase activity of Kin5(WT) and Kin5(SC) was monitored in the absence and presence of microtubules (MTs)[17]. For Kin5(WT), the maximum rate of MgATP turnover was similar to that of MnATP in both the absence and presence of MTs (Fig. 3a,b, respectively). For Kin5(SC), however, the rate of MgATP turnover showed between 83–94 percent reduction, but could be rescued to WT levels with MnATP. At a high metal concentration (5 mM), the ATPase activity of Kin5(SC) could be controlled by varying the $[Mn^{2+}]/[Mg^{2+}]$ ratio in the absence (Fig. 3c) or presence (Fig. 3d) of MTs.

### Metal rescue observed for divergent kinesin motors

To test this metal rescue in other members of the kinesin superfamily, the corresponding switch 1 serine was substituted with cysteine in the motor domain of *Homo sapiens* kinesin-1 (Kin1 or conventional kinesin), *D. melanogaster* kinesin-10 (Kin10 or Nod), and *D. melanogaster* kinesin-14 (Kin14 or Ncd) (Supplementary Table 1). These well-characterized kinesins represent diverse properties of the superfamily, including different locations of the motor domain (Kin1, Kin5, Kin10 are N-terminal; Kin14 is C-terminal), differences in processivity (Kin1 and Kin5 are processive; Kin10 and Kin14 are non-processive), and differences in motility (Kin1, Kin5, Kin14 are motile; Kin10 is non-motile). Metal rescue was observed for all kinesins tested (Fig. 3e–g), indicating that this phenomenon was found throughout the superfamily and that metal-based control of the catalytic activity of specific kinesin motors is feasible.

### ATP hydrolysis reaction affected by switch 1 substitution

Acid-quench experiments were performed to measure the presteady-state kinetics of MgATP and MnATP hydrolysis in order to determine which step of the mechanism was defective in the SC kinesin mutant. These experiments were conducted at high enzyme concentration (75 μM) to monitor phosphate production during the first and subsequent ATP hydrolysis events. If ATP hydrolysis is defective in Kin5(SC), then linear phosphate production over time would be observed. However, if phosphate release is affected, then an exponential burst of phosphate product would be expected. Fig. 4a shows linear kinetics of phosphate formation in the presence of MgATP. However, a robust burst of phosphate production was observed for MnATP, as previously observed for Kin5(WT)[13]. These results indicate that the catalytic step of ATP hydrolysis is aberrant in the SC kinesin mutant with $Mg^{2+}$, and that hydrolysis can be rescued by $Mn^{2+}$, presumably due to stronger interaction with the cysteine.

To directly measure the kinetics of phosphate release in real time, we performed stopped-flow experiments using the MDCC-PBP assay[18]. In this coupled assay, ATP binds the active site of Kin5 followed by ATP hydrolysis. When $P_i$ is released to the solution, MDCC-PBP binds the $P_i$ rapidly and tightly resulting in a fluorescence enhancement (Fig. 4b). Similar phosphate release kinetics were observed for Kin5(WT) with MgATP and MnATP. Kin5(SC) showed a slow linear rate of $P_i$ release with $Mg^{2+}$ but this was rescued to WT levels by $Mn^{2+}$ in the absence (Fig. 4b) and presence (Fig. 4c) of MTs. The slow linear rate of $P_i$ release for Kin5(SC) with $Mg^{2+}$ was consistent with slow linear rate of ATP hydrolysis that precedes the $P_i$ release step.

### Metal rescue of microtubule gliding by mutant kinesin

Motility assays with dimeric Kin1(WT) and Kin1(SC) were undertaken to determine whether the SC mutant motor promotes MT gliding *in vitro* (Supplemental Movie 1)[19]. Kin1 shows rapid and robust motility under similar conditions as our biochemical assays[19], thus it provides an excellent model system for investigating the mechanical force generation by a kinesin motor. After the Kin1 and rhodamine-labeled MTs were perfused into a microscope cover glass chamber, MT gliding was initiated by addition of MgATP or MnATP. MT movement of 37 ± 9 and 29 ± 8 μm/min (mean ± s.d.) was found for Kin1(WT) with $Mg^{2+}$ and $Mn^{2+}$, respectively (Fig. 5a; Supplementary Table 2). However, Kin1(SC) showed very slow motility of 0.4 ± 0.2 μm/min with $Mg^{2+}$ (Supplemental Movie 2), and partial rescue to 3.5 ± 1.4 μm/min by $Mn^{2+}$ (Fig. 5b). Lack of full rescue to WT velocity could be due to slower ATPase activity for Kin1(SC) with MnATP (Fig. 5c), but cooperativity between the two motor domains could also be altered. Nevertheless, these results demonstrate that $Mn^{2+}$ is able to rescue MT-based motility for the SC kinesin mutant.

## DISCUSSION

We have defined the minimal kinesin ATPase mechanism in the presence of different divalent metals when the conserved switch 1 serine was substituted with cysteine. This analysis has revealed a direct link between the switch 1 serine interaction with the metal and the hydrolytic step in the cycle. When this switch 1 serine was substituted with cysteine, its interaction with $Mg^{2+}$ was presumed to be weakened due to sulfur being a poorer ligand for the hard $Mg^{2+}$ ion. Very slow ATP hydrolysis was observed for the cysteine mutants of all kinesins tested, both in the absence and presence of MTs, suggesting that the mutant enzymes still possess the ability to catalyze ATP hydrolysis, albeit at a markedly reduced rate. However, normal hydrolysis rates were found for the SC mutant with $Mn^{2+}$ due to stronger interaction of sulfur with this softer metal ion.

### $Mn^{2+}$ capable of replacing $Mg^{2+}$ for kinesin

$Mg^{2+}$ and $Mn^{2+}$ share several chemical properties, including ionic radius and preferred octahedral coordination geometry, yet they differ in electronegativity, charge density and polarizability. For many $Mg^{2+}$-dependent ATPases, $Mn^{2+}$ is a suitable alternative metal cofactor for their biochemical reactions. We provide a high resolution structure of Kin10(WT) bound to MnADP, and comparison of this structure with the MgADP state[14] reveals that there is virtually no difference between the structures. These structural data are consistent with ATPase measurements that show very similar rates of ATP turnover for (WT) kinesin with $Mg^{2+}$ or $Mn^{2+}$ (Fig. 2), as well as presteady-state MgADP and MnADP release experiments that show similar kinetics for mantADP release from Kin5(WT) and Kin5(SC) in the absence and presence of MTs (Supplementary Fig. 3). Together, results presented in this study are consistent with $Mn^{2+}$ structurally and functionally replacing $Mg^{2+}$ as a metal cofactor for ATP hydrolysis in kinesin motors.

### Switch 1-metal interaction during kinesin ATPase cycle

It is commonly thought that switch 1 must close around the nucleotide to reach the hydrolysis-competent state[15]. A key interaction that occurs during switch 1 closure is

coordination of the central serine (NxxS**S**R) to the metal in the active site. When non-hydrolyzable nucleotide analogues are bound to myosin[20] and kinesin[15], as well as small G-proteins[21], this closed switch 1 conformation has been observed with the conserved switch 1 serine (or threonine for G-proteins) coordinated to the metal. In kinesins, a recent study by Parke *et al.*[15] revealed many new insights into the mechanism of ATP hydrolysis by kinesins. Although the "two-waters mechanism" proposed by Parke *et al.* seems highly favorable, the research presented in this manuscript does not directly address this hypothesis. However, we believe the metal coordination plays a key role in establishing the proper conformation of the kinesin active site for ATP hydrolysis to occur rapidly. Not only does the switch 1 serine coordinate the metal in the ATP hydrolysis-competent state, but the preceding switch 1 serine (**S**SRSH) hydrogen bonds to the γ-phosphate of the nucleotide, the polypeptide backbone makes critical interactions with the γ-phosphate and nucleophilic water, and the switch 1 arginine forms a salt bridge with the conserved switch 2 glutamic acid. Our results support the hypothesis that switch 1 serine coordination of the metal represents the keystone interaction that facilitates rapid closure of Sw1 to promote rapid ATP hydrolysis.

One explanation for our results has switch 1 in the SC mutant remaining predominantly in the open conformation upon ATP binding, and thus not coordinating the $Mg^{2+}$. This open switch 1 conformation in the presence of $Mg^{2+}$ would explain the very slow hydrolysis rate. However, in the presence of $Mn^{2+}$, switch 1 can close through its interaction with this metal and achieve the ATP-hydrolysis competent state. Alternatively, switch 1 in the SC mutant does close upon ATP binding and the cysteine coordinates the $Mg^{2+}$, but the sulfur–$Mg^{2+}$ interaction modulates the Lewis acidity of the $Mg^{2+}$ thereby altering the phosphate charge density required for rapid hydrolysis. When $Mn^{2+}$ is substituted as the metal cofactor, the electrostatics in the active site are restored, and thus the kinetics of the hydrolysis reaction are rescued. Future investigations will be directed to test these hypotheses.

### Switch 1 as "sensor" for productive kinesin-1 stepping

We performed *in vitro* MT gliding assays using dimeric kinesin-1 WT and SC in the presence of $Mg^{2+}$ and $Mn^{2+}$. For WT, we saw comparable MT gliding rates with either metal and the observed rate was similar to previously published work[19]. For SC in the presence of $Mg^{2+}$, we observed very slow MT motility (~two orders of magnitude reduction compared to WT), even though we only measured an ~order of magnitude reduction in MgATPase rate. However, upon addition of $Mn^{2+}$, we observed an ~order of magnitude enhancement of both MT motility and MnATPase activity. Since we utilized an ATP-regeneration system and performed these experiments at high ATP concentration (5 mM), these results are likely not associated with weaker binding of ATP to SC. This result was dependent neither on motor density on the surface of the coverslip (half concentration and double concentration tested) nor on the length of MTs used (shorter MTs showed a comparable rate as longer MTs) nor on the specific protein preparation used (n=2). We propose that a switch 1 conformational change during the kinesin-1 ATPase cycle plays a critical role in coupling ATPase activity in the motor to productive force production that leads to stepping of the motor along the MT. Future studies using dimeric kinesin-5 and

kinesin-10 SC mutants will determine if this phenomenon is common to processive motors (kinesin-1 and kinesin-5) or is shared among non-processive motors as well (kinesin-14).

## Potential Broad Applications

To the best of our knowledge, this is first demonstration of metal rescue in a protein-based hydrolytic enzyme. Given the generality of this metal rescue approach across the kinesin family, it should be applicable to other nucleotide triphosphorylase (NTPase) systems, including myosins and G-proteins. Currently, one of the most powerful chemical-genetic methods available involves an approach pioneered by Shokat and colleagues in which a protein kinase target is mutated to create an additional pocket in the nucleotide binding region such that an inhibitor resembling a nucleotide with a bulky side group can be accommodated[22,23]. While such stable mutants have been successfully created in a number of different systems[24,25], in proteins that do not tolerate introduction of an additional cavity, a potential advantage of the metal rescue technique is that it only requires a conservative serine to cysteine mutation, which is unlikely to have an effect on the structure of the target enzyme. A further distinction between the two approaches is that the metal rescue does not require inhibitors or modified nucleotides; one can simply vary the ratio of Mg2+ and Mn2+ ions, which in turn can modulate target enzyme activity from inactive to wild type levels. Additionally, the ability to alter serine residues in different regions of the active site allows one to inhibit different steps in the catalytic cycle of an enzyme, thereby dissecting its mechanism. For example, while conserved serines in the P-loop are critical for nucleotide binding, the switch 1 serine affects nucleotide hydrolysis without affecting binding, as demonstrated in this work.

There are several relevant and important applications of our metal switch approach that will substantially impact the molecular motor community as well as more broadly to the P-loop NTPase research community. Examples of such applications include using the metal switch to control the activity of a single catalytic head of a dimeric motor (e.g. kinesin-1, myosin-5) to investigate biophysical questions of inter-molecular head-head communication, mechanical versus chemical gating, and motor stepping behavior. The metal switch could also be utilized to control the activity of a single type of molecular motor in multiple motor assays to distinguish the distinct roles of various motors involved in cytoskeletal structures (e.g. reconstituted mitotic spindles). Ultimately, this technology could be incorporated into the development of an *in vivo* system that tolerates high concentrations of $Mn^{2+}$ (e.g. *Saccharomyces cerevisiae*[26]) to study various cell biological phenomena. Given the structural similarity between molecular motors (e.g. kinesins and myosins) and molecular switch proteins (e.g. small G-proteins), such a metal switch should work in other NTPase systems to provide a way to control their activity *in vitro* and *in vivo*. Finally, the substitution of the conserved P-loop serine or threonine (consensus: GxxxxGKS/T) with a cysteine could provide for metal rescue of nucleotide binding and hence restoration of activity in P-loop containing hydrolases (EC 3.6). This protein mega-family is made up of at least 10 superfamilies representing tens-of-thousands of enzymes found in virtually all biological systems.

## Supplementary Material

Refer to Web version on PubMed Central for supplementary material.

## ACKNOWLEDGEMENTS

We thank V. Stojanoff of the National Synchrotron Light Source beam line X6A for help with data collection, R. Sloboda, A. Lavanway, and H. Sardar for help with the fluorescence microscopy and W. Casey for electron paramagnetic resonance training. The project was supported by F32AR054653 from the National Institutes of Health (National Institute of General Medical Sciences) to J.C.C. and research carried out at the X6A beam line was funded by the National Institutes of Health (National Institute of General Medical Sciences) under agreement GM-0080. The National Synchrotron Light Source at Brookhaven National Laboratory is supported by the United States Department of Energy under contract DE-AC02-98CH10886.

## ABBREVIATIONS

| | |
|---|---|
| **MT** | microtubule |
| **P-loop** | phosphate binding loop |
| **WT** | wild-type |
| **SC** | serine-to-cysteine substitution |
| **EPR** | electron paramagnetic resonance |
| **MDCC-PBP** | coumarin-labeled phosphate binding protein |

## REFERENCES

1. Saraste M, Sibbald PR, Wittinghofer A. The P-loop--a common motif in ATP- and GTP-binding proteins. Trends Biochem Sci. 1990; 15:430–434. [PubMed: 2126155]
2. Vale RD. Switches, latches, and amplifiers: common themes of G proteins and molecular motors. J Cell Biol. 1996; 135:291–302. [PubMed: 8896589]
3. Marx A, Muller J, Mandelkow E. The structure of microtubule motor proteins. Adv Protein Chem. 2005; 71:299–344. [PubMed: 16230115]
4. Frederiksen JK, Piccirilli JA. Identification of catalytic metal ion ligands in ribozymes. Methods. 2009; 49:148–166. [PubMed: 19651216]
5. Piccirilli JA, Vyle JS, Caruthers MH, Cech TR. Metal ion catalysis in the Tetrahymena ribozyme reaction. Nature. 1993; 361:85–88. [PubMed: 8421499]
6. Warnecke JM, Furste JP, Hardt WD, Erdmann VA, Hartmann RK. Ribonuclease P (RNase P) RNA is converted to a Cd(2+)-ribozyme by a single Rp-phosphorothioate modification in the precursor tRNA at the RNase P cleavage site. Proc Natl Acad Sci U S A. 1996; 93:8924–8928. [PubMed: 8799129]
7. Peracchi A, Beigelman L, Scott EC, Uhlenbeck OC, Herschlag D. Involvement of a specific metal ion in the transition of the hammerhead ribozyme to its catalytic conformation. J Biol Chem. 1997; 272:26822–26826. [PubMed: 9341112]
8. Sontheimer EJ, Sun S, Piccirilli JA. Metal ion catalysis during splicing of premessenger RNA. Nature. 1997; 388:801–805. [PubMed: 9285595]
9. Sarnovsky RJ, May EW, Craig NL. The Tn7 transposase is a heteromeric complex in which DNA breakage and joining activities are distributed between different gene products. Embo J. 1996; 15:6348–6361. [PubMed: 8947057]
10. Allingham JS, Pribil PA, Haniford DB. All three residues of the Tn 10 transposase DDE catalytic triad function in divalent metal ion binding. J Mol Biol. 1999; 289:1195–1206. [PubMed: 10373361]

11. Gao K, Wong S, Bushman F. Metal binding by the D,DX35E motif of human immunodeficiency virus type 1 integrase: selective rescue of Cys substitutions by Mn2+ in vitro. J Virol. 2004; 78:6715–6722. [PubMed: 15194746]
12. Jaffe EK, Cohn M. Diastereomers of the nucleoside phosphorothioates as probes of the structure of the metal nucleotide substrates and of the nucleotide binding site of yeast hexokinase. J Biol Chem. 1979; 254:10839–10845. [PubMed: 387756]
13. Cochran JC, Gilbert SP. ATPase mechanism of Eg5 in the absence of microtubules: insight into microtubule activation and allosteric inhibition by monastrol. Biochemistry. 2005; 44:16633–16648. [PubMed: 16342954]
14. Cochran JC, et al. ATPase cycle of the nonmotile kinesin NOD allows microtubule end tracking and drives chromosome movement. Cell. 2009; 136:110–122. [PubMed: 19135893]
15. Parke CL, Wojcik EJ, Kim S, Worthylake DK. ATP hydrolysis in Eg5 kinesin involves a catalytic two-water mechanism. J Biol Chem. 2010; 285:5859–5867. [PubMed: 20018897]
16. Reed, GH.; Markham, GD. EPR of Mn(II) Complexes with Enzymes and Other Proteins. In: Berliner, LJ.; Reuben, J., editors. Biological Magnetic Resonance. Plenum, NY: 1984. p. 73-142.
17. Leonard M, Song BD, Ramachandran R, Schmid SL. Robust colorimetric assays for dynamin's basal and stimulated GTPase activities. Methods Enzymol. 2005; 404:490–503. [PubMed: 16413294]
18. Brune M, Hunter JL, Corrie JE, Webb MR. Direct, real-time measurement of rapid inorganic phosphate release using a novel fluorescent probe and its application to actomyosin subfragment 1 ATPase. Biochemistry. 1994; 33:8262–8271. [PubMed: 8031761]
19. Woehlke G, et al. Microtubule interaction site of the kinesin motor. Cell. 1997; 90:207–216. [PubMed: 9244295]
20. Fisher AJ, et al. X-ray structures of the myosin motor domain of Dictyostelium discoideum complexed with MgADP.BeFx and MgADP.AlF. Biochemistry. 1995; 34:8960–8972. [PubMed: 7619795]
21. Pai EF, et al. Refined crystal structure of the triphosphate conformation of H-ras p21 at 1.35 A resolution: implications for the mechanism of GTP hydrolysis. Embo J. 1990; 9:2351–2359. [PubMed: 2196171]
22. Shah K, Liu Y, Deirmengian C, Shokat KM. Engineering unnatural nucleotide specificity for Rous sarcoma virus tyrosine kinase to uniquely label its direct substrates. Proc Natl Acad Sci U S A. 1997; 94:3565–3570. [PubMed: 9108016]
23. Bishop AC, et al. Design of allele-specific inhibitors to probe protein kinase signaling. Curr Biol. 1998; 8:257–266. [PubMed: 9501066]
24. Shogren-Knaak MA, Alaimo PJ, Shokat KM. Recent advances in chemical approaches to the study of biological systems. Annu Rev Cell Dev Biol. 2001; 17:405–433. [PubMed: 11687495]
25. Specht KM, Shokat KM. The emerging power of chemical genetics. Curr Opin Cell Biol. 2002; 14:155–159. [PubMed: 11891113]
26. Reddi AR, Jensen LT, Culotta VC. Manganese homeostasis in Saccharomyces cerevisiae. Chem Rev. 2009; 109:4722–4732. [PubMed: 19705825]
27. Bauer CB, Holden HM, Thoden JB, Smith R, Rayment I. X-ray structures of the apo and MgATP-bound states of Dictyostelium discoideum myosin motor domain. J Biol Chem. 2000; 275:38494–38499. [PubMed: 10954715]
28. Kull FJ, Sablin EP, Lau R, Fletterick RJ, Vale RD. Crystal structure of the kinesin motor domain reveals a structural similarity to myosin. Nature. 1996; 380:550–555. [PubMed: 8606779]
29. Maliga Z, Kapoor TM, Mitchison TJ. Evidence that monastrol is an allosteric inhibitor of the mitotic kinesin Eg. Chem Biol. 2002; 9:989–996. [PubMed: 12323373]
30. Cui W, et al. Drosophila Nod protein binds preferentially to the plus ends of microtubules and promotes microtubule polymerization in vitro. Mol Biol Cell. 2005; 16:5400–5409. [PubMed: 16148044]
31. Chandra R, Salmon ED, Erickson HP, Lockhart A, Endow SA. Structural and functional domains of the Drosophila ncd microtubule motor protein. J Biol Chem. 1993; 268:9005–9013. [PubMed: 8473343]

32. Kabsch W. Automatic processing of rotation diffraction data from crystals of initially unknown symmetry and cell constants. J. Appl. Cryst. 1993; 26:795–800.

33. Brunger AT, et al. Crystallography & NMR system: A new software suite for macromolecular structure determination. Acta Crystallogr D Biol Crystallogr. 1998; 54:905–921. [PubMed: 9757107]

34. Gilbert SP, Mackey AT. Kinetics: a tool to study molecular motors. Methods. 2000; 22:337–354. [PubMed: 11133240]

35. Cochran JC, Krzysiak TC, Gilbert SP. Pathway of ATP hydrolysis by monomeric kinesin Eg. Biochemistry. 2006; 45:12334–12344. [PubMed: 17014086]

36. Hyman A, et al. Preparations of modified tubulins. Meth. Enzymol. 1990; 196:303–319.

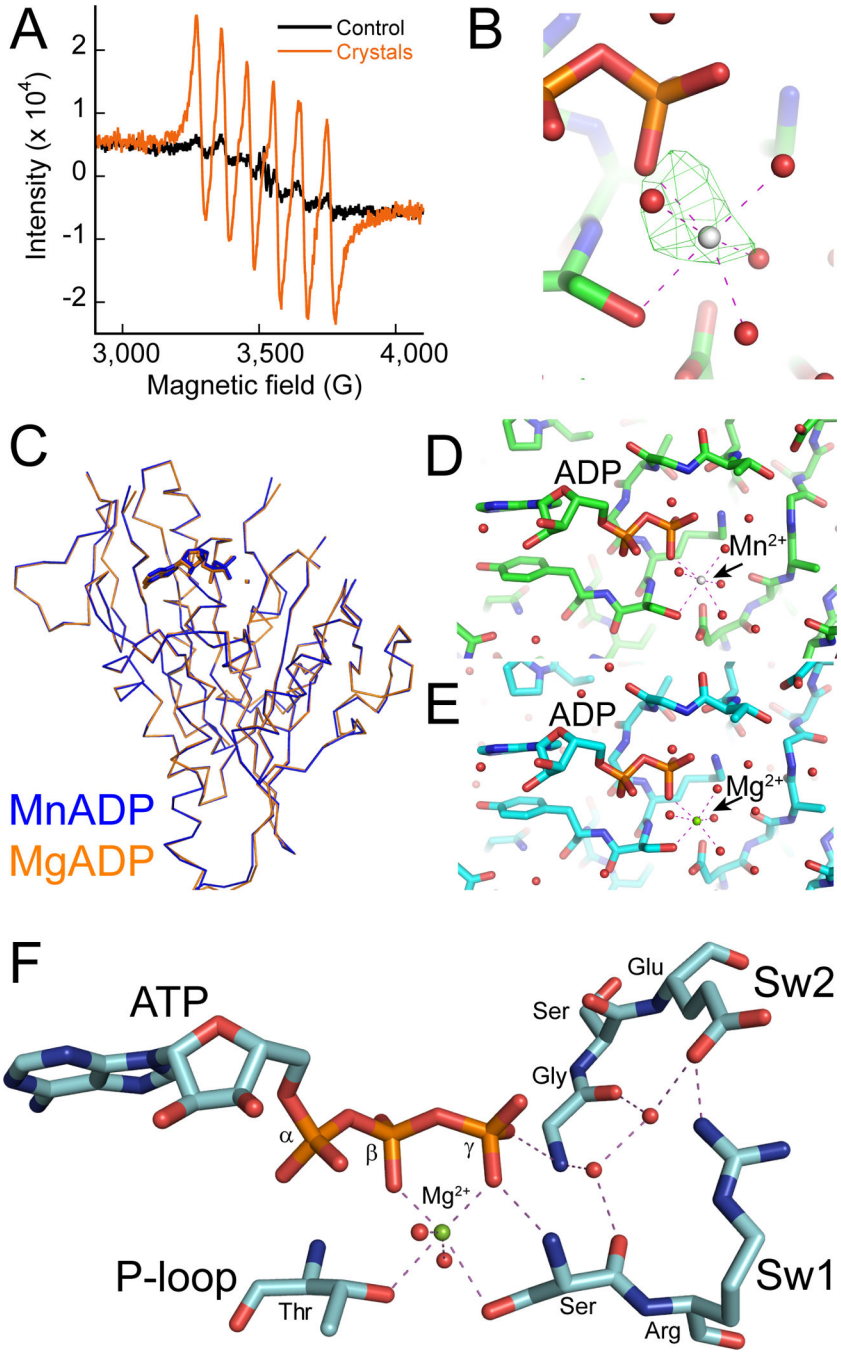


**Figure 1.**

Crystal structure of Kin10•MnADP and the ATP hydrolysis-competent state for kinesin. (**a**) EPR spectra of washed and denatured Kin10•MnADP crystals and mock control (no crystals) are shown. (**b**) The active site of Kin10•MnADP is shown. Water molecules are shown as red spheres and $Mn^{2+}$ as gray sphere. The green cage represents the positive peak in the $F_oF_c$ map (3 σ) with the MnADP data being refined with the Kin10•MgADP structure (3DC4). (**c**) Alignment of main chain atoms of Kin10•MnADP with Kin10•MgADP. (**d,e**) Shown are detailed views of the active site of Kin10•MnADP and Kin10•MgADP,

respectively. $Mg^{2+}$ is shown as a green sphere. (**f**) Model of the ATP hydrolysis-competent state of kinesin. AMPPNP from the Kin5 structure [3HQD; [15]] was replaced with ATP from Myo2 structure [1FMW; [27]] after alignment using the P-loop residues.

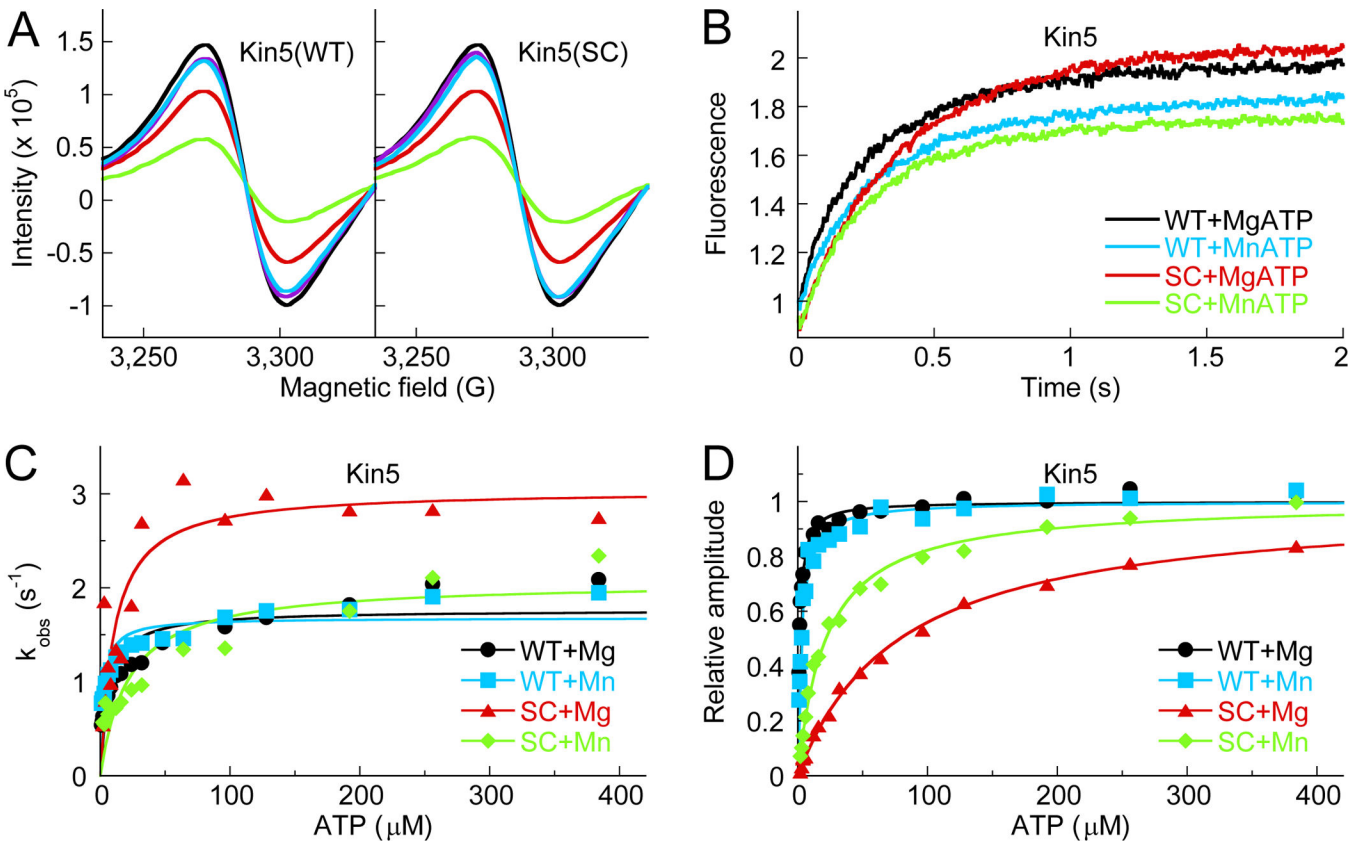


**Figure 2.**

Metal and nucleotide binding to kinesin. (**a**) Partial $Mn^{2+}$ EPR spectra for Kin5(WT) and Kin5(SC) under various conditions: $Mn^{2+}$ alone (black), $Mn^{2+}$ and nucleotide-free Kin5 (cyan), MnADP (red), MnADP plus Kin5 (green), and Kin5•MnADP plus excess $Mg^{2+}$ (purple). Final concentrations: 50 μM $MnCl_2$, 50 μM ADP, 50 μM Kin5, 5 mM $MgCl_2$. (**b**) Tryptophan fluorescence enhancement of Kin5(WT) and Kin5(SC) upon rapid mixing in a stopped-flow instrument with MgATP or MnATP (as indicated). Final concentrations: 5 μM Kin5, 500 μM ATP, 5 mM $MgCl_2$ or $MnCl_2$. (**c**) Observed rates of each fluorescent transient were plotted against ATP concentration. Each data set was fit to a hyperbola to determine the $K_{d,ATP}$ (mean ± s.e.m.): WT+$Mg^{2+}$ = 6.2 ± 1.4 μM; WT+$Mn^{2+}$ = 2.5 ± 0.5 μM; SC +$Mg^{2+}$ = 10.4 ± 3.2 μM; SC+$Mn^{2+}$ = 21.8 ± 7.0 μM. (**d**) Relative amplitudes were plotted as a function of ATP concentration. The data were fit to a hyperbola: WT+$Mg^{2+}$ = 1.4 ± 0.1 μM; WT+$Mn^{2+}$ = 2.7 ± 0.2 μM; SC+$Mg^{2+}$ = 78.6 ± 4.4 μM; SC+$Mn^{2+}$ = 21.6 ± 1.5 μM.

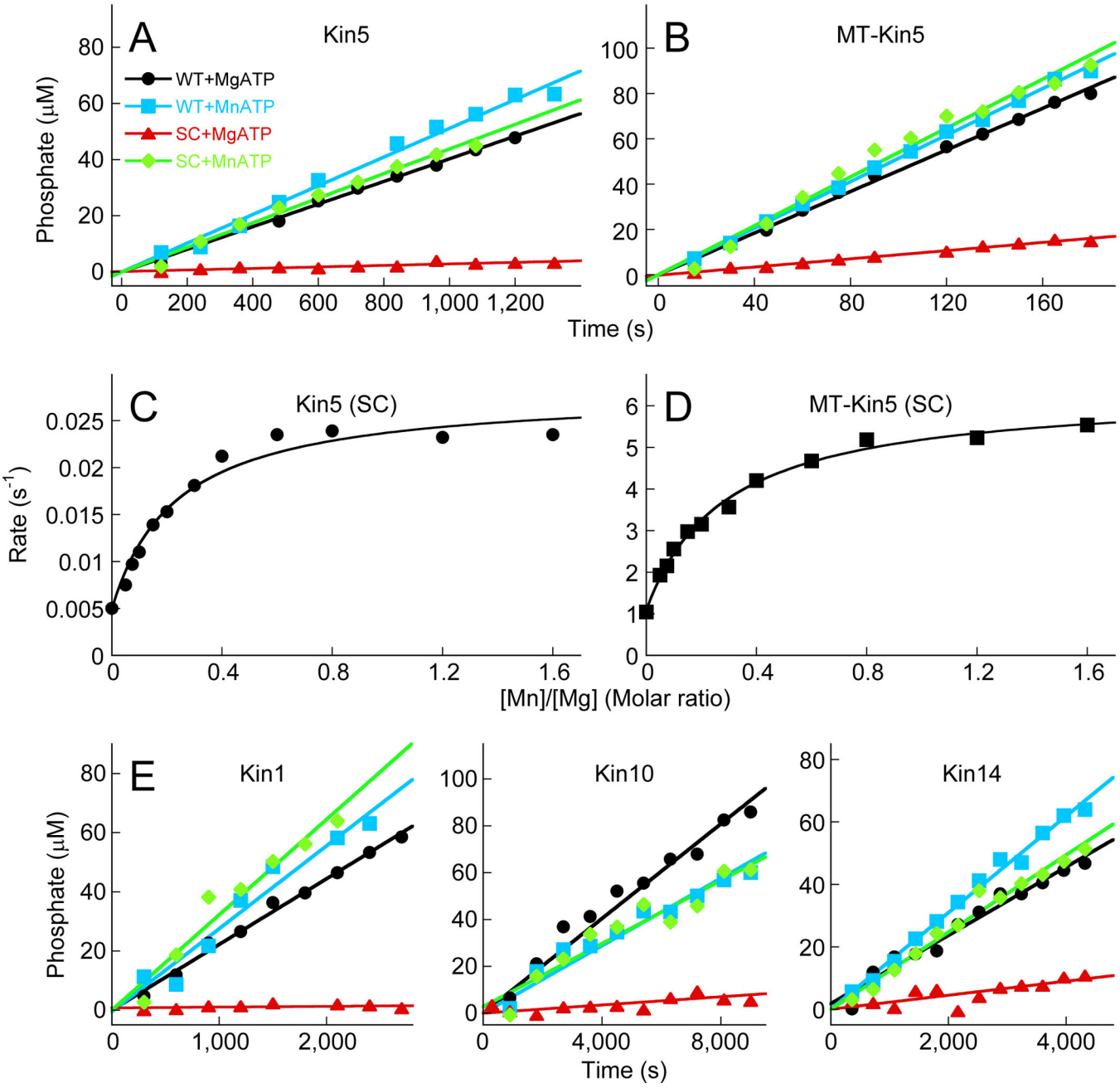


**Figure 3.**

$Mn^{2+}$ rescue of kinesin (SC) ATPase in the absence and presence of MTs. (**a**) Time course of MgATP and MnATP hydrolysis by Kin5(WT) and Kin5(SC) in the absence of MTs and (**b**) in the presence of MTs. Final concentrations: 0.5 μM Kin5 (no MTs), 50 nM Kin5 plus 2 μM MTs, 5 μM taxol, 200 μM ATP, 5 mM $MgCl_2$ or $MnCl_2$. (**c,d**) The observed rate of ATP hydrolysis for Kin5(SC) plotted against $[Mn^{2+}]/[Mg^{2+}]$ ratio in the absence and presence of MTs. (**e**) Time course of MgATP and MnATP hydrolysis by Kin1, Kin10, and Kin14 as indicated. Final concentrations: 4 μM Kin1, 10 μM Kin10, 10 μM Kin14, 200 μM ATP. Representative data shown for n=3 experiments for each time course.

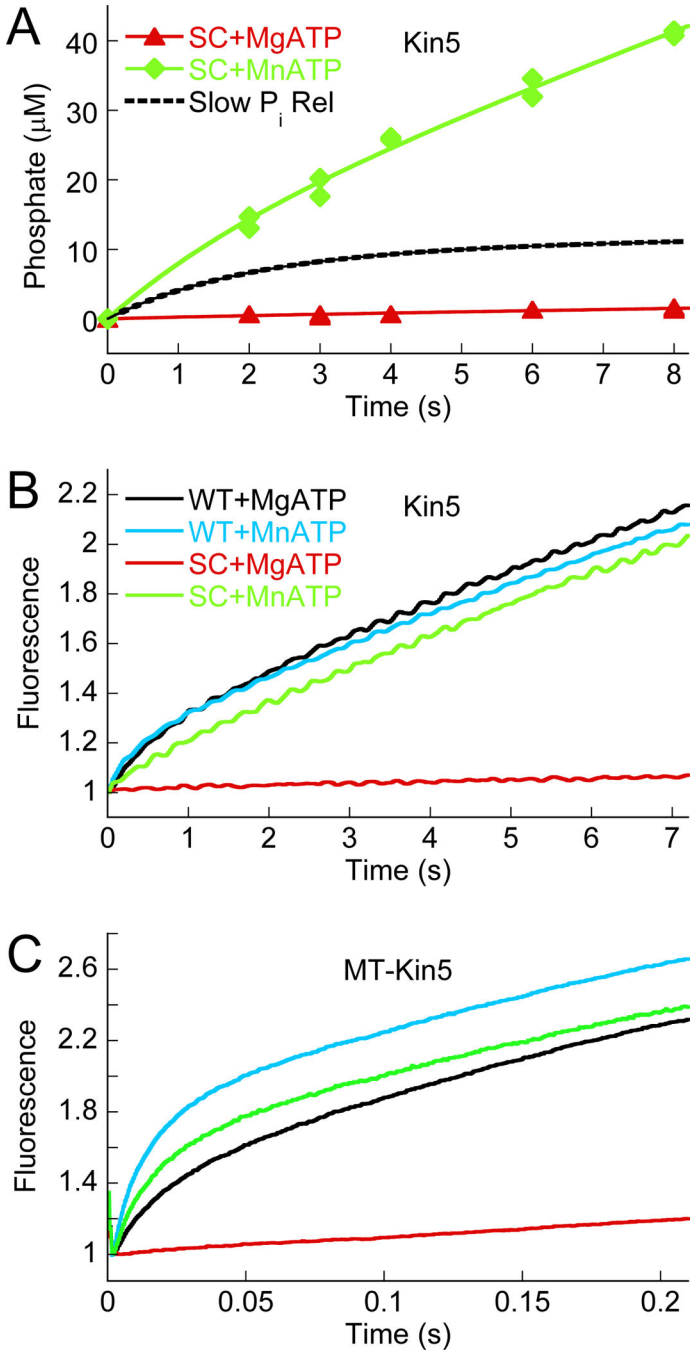


**Figure 4.**

Acid-quench and phosphate release kinetics. (**a**) Acid quench kinetics of phosphate product formation by Kin5(SC) with MgATP and MnATP (as indicated). Dash line corresponds to expected kinetics if the phosphate release step were slowed. Final concentrations: 75 μM Kin5, 200 μM ATP, 5 mM $MgCl_2$ or $MnCl_2$. (**b,c**) Phosphate release kinetics by Kin5(WT) and Kin5(SC) with MgATP and MnATP in the absence and presence of MTs using the MDCC-PBP coupled assay. Final concentrations: 1 μM Kin5, 0 or 2 μM MTs, 0 or 5 μM

taxol, 10 μM MDCC-PBP, 0.05 U/ml PNPase, 75 μM MEG, 200 μM ATP, 5 mM $MgCl_2$ or $MnCl_2$.

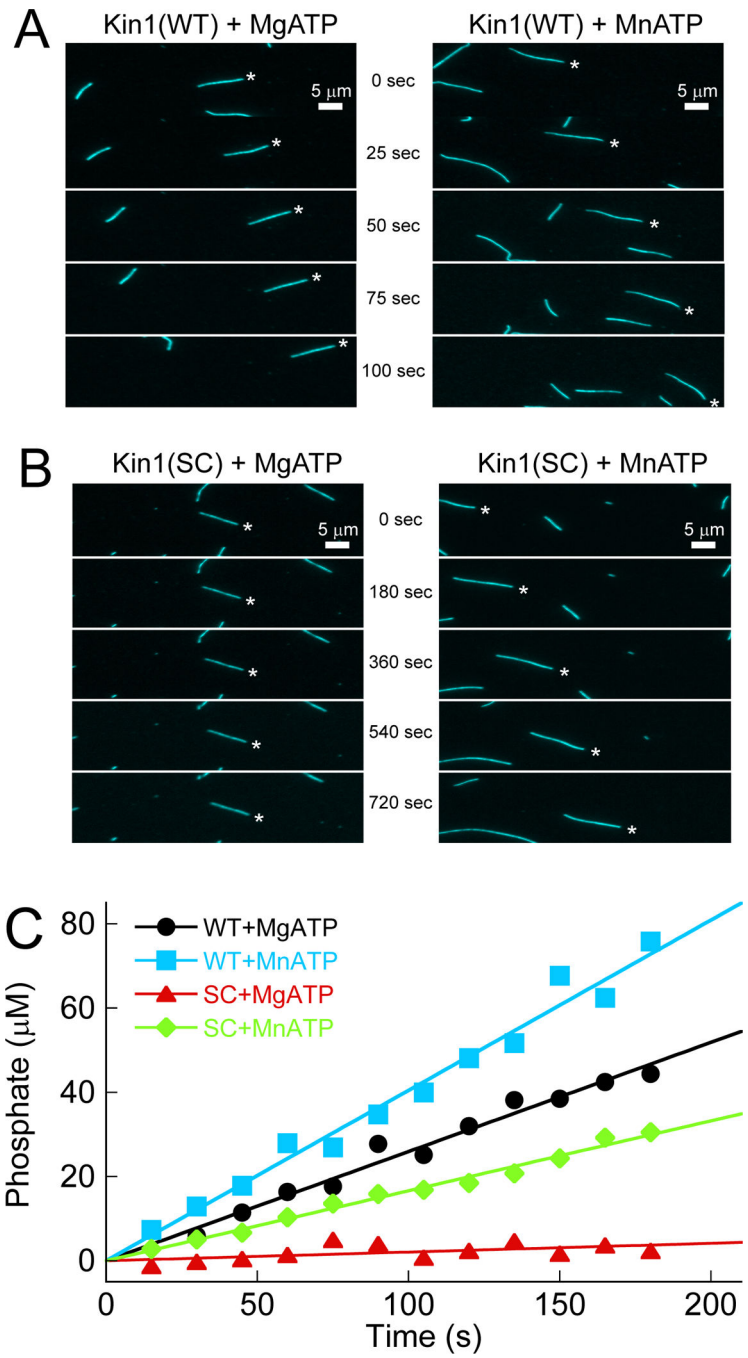


**Figure 5.**

$Mn^{2+}$ rescue of *in vitro* MT gliding. (**a,b**) Dimeric Kin1(WT) and dimeric Kin1(SC) promoted MT gliding in MgATP and MnATP. Asterisk highlights leading MT end. (**c**) Time course of MgATP and MnATP hydrolysis by dimeric Kin1(WT) and Kin1(SC) in the presence of MTs. Final concentrations: 10 nM Kin1, 2 μM MTs, 5 μM taxol, 200 μM ATP, 5 mM $MgCl_2$ or $MnCl_2$. WT+$Mg^{2+}$ (mean ± s.e.m.): 25.9 ± 1.5 $s^{-1}$, WT+$Mn^{2+}$: 40.4 ± 1.9

$s^{-1}$, SC+$Mg^{2+}$: 2.1 ± 0.9 $s^{-1}$, and SC+$Mn^{2+}$: 16.6 ± 0.6 $s^{-1}$. Representative data shown for n=3 experiments for each time course.

## TABLE 1

Data collection and refinement statistics.

| | MnADP [a] |
|---|---|
| **Data Collection** | |
| Space Group | $P2_12_12_1$ |
| Cell Dimensions | |
| *a*, *b*, *c* (Å) | 47.6, 75.7, 94.2 |
| α, β, γ,(°) | 90, 90, 90 |
| Resolution (Å) | 20-2.6 (2.76-2.60) |
| $R_{sym}$ (%) [b,c] | 9.4 (42.9) |
| $I / \sigma(I)$ [b] | 24.5 (4.3) |
| Completeness (%) [b] | 99.8 (99.9) |
| Redundancy [b] | 7.10 (7.22) |
| **Refinement** | |
| Resolution (Å) | 20 – 2.6 |
| No. Reflections [b] | 77485 (15497) |
| $R_{work}$ / $R_{free}$ [d] (%) | 22.7 / 27.0 |
| No. atoms | |
| Protein | 2247 |
| Ligand/ion | 29 |
| Water | 28 |
| *B*-factors | |
| Protein | 32.7 |
| Ligand/ion | 25.9 |
| Water | 44.7 |
| R.M.S. Deviations | |
| Bond Length (Å) | 0.009 |
| Bond Angle (°) | 1.3 |

[a] PDB ID is 3PXN. One crystal used for structure determination.

[b] Data in parentheses represent the highest resolution shell.

[c] $R_{sym} = 100 \times \Sigma_h\Sigma_i \mid I(h) - I_i(h) \mid / \Sigma_h\Sigma_i I_i(h)$, where $I_i(h)$ and $I(h)$ values are the *i*th and mean measurements of the intensity of reflection *h*.

[d] $R_{free}$ is for 5 % of total reflections not included in the refinement.